JVI Journals.ASM.org

Increased Antibody Affinity Confers Broad *In Vitro* Protection against Escape Mutants of Severe Acute Respiratory Syndrome Coronavirus

Mridula Rani,[a] Meagan Bolles,[f] Eric F. Donaldson,[e] Thomas Van Blarcom,[b] Ralph Baric,[e] Brent Iverson,[a,c] and George Georgiou[a,b,d]

Institute of Cellular and Molecular Biology,[a] Department of Chemical Engineering,[b] Department of Chemistry and Biochemistry,[c] and Department of Molecular Genetics and Microbiology,[d] The University of Texas at Austin, Austin, Texas, USA; Department of Epidemiology, School of Public Health, University of North Carolina at Chapel Hill, Chapel Hill, North Carolina, USA[e]; and Department of Microbiology and Immunology, University of North Carolina at Chapel Hill, Chapel Hill, North Carolina, USA[f]

Even though the effect of antibody affinity on neutralization potency is well documented, surprisingly, its impact on neutralization breadth and escape has not been systematically determined. Here, random mutagenesis and DNA shuffling of the single-chain variable fragment of the neutralizing antibody 80R followed by bacterial display screening using anchored periplasmic expression (APEx) were used to generate a number of higher-affinity variants of the severe acute respiratory syndrome coronavirus (SARS-CoV)-neutralizing antibody 80R with equilibrium dissociation constants (K_D) as low as 37 pM, a >270-fold improvement relative to that of the parental 80R single-chain variable fragment (scFv). As expected, antigen affinity was shown to correlate directly with neutralization potency toward the icUrbani strain of SARS-CoV. Additionally, the highest-affinity antibody fragment displayed 10-fold-increased broad neutralization *in vitro* and completely protected against several SARS-CoV strains containing substitutions associated with antibody escape. Importantly, higher affinity also led to the suppression of viral escape mutants *in vitro*. Escape from the highest-affinity variant required reduced selective pressure and multiple substitutions in the binding epitope. Collectively, these results support the hypothesis that engineered antibodies with picomolar dissociation constants for a neutralizing epitope can confer escape-resistant protection.

Coronavirus-mediated severe acute respiratory syndrome (SARS) emerged from zoonotic reservoirs and caused epidemic disease outbreaks in late 2002 and early 2003 that posed a threat to public health worldwide. The disease is characterized by a rapidly progressive atypical pneumonia, and the causative agent was identified as a novel group 2b coronavirus (SARS-CoV) (16). Though the disease is now largely contained, a few sporadic cases were reported in late 2003 and 2004 that were caused by different isolates of SARS-CoV (15).

SARS-CoV is an enveloped, single-stranded positive-sense RNA virus that infects the host cell via the binding of the spike (S) glycoprotein of the viral envelope to the ACE2 (angiotensin-converting enzyme 2) receptor of the host cell (3, 13). The receptor-binding domain (RBD), a 193-amino-acid fragment located in the S1 region of the S protein, is responsible for the initial binding event (3). Sequence analyses of different SARS-CoV isolates have revealed that the RBD is subject to strong selective pressure by antibody immune responses in the host. Amino acid substitutions within the RBD have played a major role in the ability of SARS-CoVs to overcome the species barrier, initially allowing animal-to-human transmission and subsequent adaptation to transmission among humans (39).

The high immunogenicity of the S protein as well as its crucial role in the recognition of the host cell receptor and the initiation of infection has made it an important target for both vaccine and therapeutic development (3). Several monoclonal antibodies (MAbs) to the S protein have been developed and shown to protect against SARS-CoV infection *in vitro* (18, 32). Additionally, a variety of neutralizing antibodies (7, 20, 27, 44) have been shown to confer protection in a mouse model. The best characterized of these neutralizing antibodies, 80R, was isolated from a large naïve human single-chain variable fragment (scFv) library using phage display. 80R binds the S protein with a reported equilibrium dissociation constant (K_D) equal to 32 nM while recognizing a conformational epitope that overlaps the RBD in the S1 domain (28). However, antibody-mediated selective pressure *in vitro* is known to result in antigenic drift within the RBD, leading to the accumulation of mutations that abolish neutralization by 80R (26).

Various strategies have been explored for developing broadly neutralizing antibodies that can both protect against heterovariant SARS-CoV strains present in the natural reservoirs and hinder the generation of escape mutants when the virus is challenged with the neutralizing antibody. Rockx et al. and ter Meulen et al. achieved broader neutralization against SARS-CoV escape mutants using a combination of two monoclonal antibodies that recognize nonoverlapping neutralizing epitopes on the S protein (20, 29). Rockx et al. were successful in isolating four broadly neutralizing antibodies from human memory B cells that neutralized both zoonotic and human strains, and a cocktail of these antibodies was proposed as a means for providing better protection against infection (21). However, the development of a therapeutic strategy comprising two or more recombinant antibodies raises serious practical concerns. As an alternative, Sui and coworkers engineered variants of the 80R scFv by structure-guided randomization of key residues in the Vκ light chain. The resulting library was screened by phage display toward the S protein RBD containing the dominant mutations found in escape variants (D480A or D480G) from human SARS-CoV isolates (26). Two antibody variants, fm6 and fm39, were shown to be broadly neutralizing in an *in vitro* neutralization assay with pseudotyped virus containing the

Received 1 February 2012 **Accepted** 6 June 2012
Published ahead of print 13 June 2012
Address correspondence to George Georgiou, gg@che.utexas.edu.

doi:10.1128/JVI.00233-12

Tor2 or GD03 strain RBD or the D480A or D480G mutation. These broadly neutralizing antibodies exhibited 10-fold-lower affinity than 80R for the Tor2 strain RBD, but unlike 80R, they also bound RBD (D480A) and RBD (D480G) with nanomolar affinity. The results of Sui et al. (26) revealed that *in vitro* selections can be used to engineer broadly neutralizing antibodies; however, they are predicated upon knowledge of the relevant escape mutations and the availability of the respective protein variants required for panning experiments.

It is well established that the potency of neutralizing antibodies for either viruses or bacterial toxins depends on affinity (17, 35, 36). Surprisingly, engineering antibodies with increased affinity has not been investigated as a strategy for conferring broader protection as a means to hinder escape. A higher antigen affinity results from a higher $\Delta G_{binding}$. While antibody-antigen interactions are often dominated by interactions with a binding "hot spot" on the antigen, a high $\Delta G_{binding}$ can also arise from additional interactions between the epitope and the paratope (14). Accordingly, we hypothesized that increasing the affinity of 80R for the RBD can elicit broader neutralization. Variants of the 80R scFv antibody fragment exhibiting up to 280-fold-higher affinity for the RBD were generated by random mutagenesis and screening using *Escherichia coli* display by anchored periplasmic expression (APEx) (9). As expected, *in vitro* neutralization potency against the icUrbani strain correlated directly with affinity. Importantly, neutralization of viruses containing the RBD D480A or D480Y mutation that evaded neutralization by 80R (28) also correlated with affinity. Only reduced selective pressure with lower concentrations of the high-affinity antibody led to the evolution of SARS-CoV escape mutants, which contained, in addition to D480Y or D480A, secondary amino acid substitutions within the 80R epitope.

MATERIALS AND METHODS

Bacterial strains and plasmids. *Escherichia coli* Jude1 (DH10B F::Tn*10*) cells (8) were used for all the cloning and protein expression experiments reported here. Plasmid pAPEx1 was used for *N*-terminal APEx display of scFv and the construction of scFv libraries (9). pMopac16 contains a *pelB* leader followed by SfiI sites used for cloning the scFv gene, a human kappa light-chain constant domain for single-chain-antibody-fragment (scAb) expression, a C-terminal 6-histidine tag for purification, and the Skp chaperone to aid soluble-protein expression in the periplasmic space (10).

Viruses and cells. Recombinant viruses icUrbani (AY278741), icGD03-MA, and icHC/SZ/61/03 were propagated in Vero E6 cells (22, 24, 38). Vero E6 was maintained in minimal essential medium (MEM) (Invitrogen, Carlsbad, CA) supplemented with 10% Fetal Clone II (HyClone, South Logan, UT) and gentamicin and kanamycin (UNC Tissue Culture Facility). Growth curves were performed in Vero E6 with the different wild-type or mutant recombinant-derived escape mutant viruses at a multiplicity of infection (MOI) of 0.1 for 1 h and overlaid with medium. Virus samples were collected at various time points postinfection and stored at −70°C until viral titers were determined by plaque assay.

Virus titers were determined as PFU by plating 6-well plates with 5×10^5 Vero E6 cells per well and inoculating cultures with 200 μl from the 10-fold serial dilutions. Cells were incubated with the virus for 1 h at 37°C and overlaid with 3 ml of 0.8% agarose in complete medium. Plates were incubated for 2 days at 37°C, and plaques were visualized by staining with neutral red for 3 to 6 h. Virus concentration was calculated as PFU/ml. All virus work was performed in a class II biological safety cabinet in a certified biosafety level 3 laboratory containing redundant exhaust fans; workers wore Tyvek suits and powered air-purifying respirators.

Construction of an scFv library. The 80R single-chain antibody gene (27) was constructed by overlap extension PCR (25). The heavy- and light-chain variable regions of the antibody were amplified by PCR, and a (Gly4Ser)4 linker was introduced by overlap extension PCR. The amplified 80R scFv PCR product was digested with SfiI and cloned into the SfiI-digested pAPEx1 vector (9) for bacterial display. The 80R scFv gene was subjected to random mutagenesis by error-prone PCR using standard protocols (6). A library of 1.6×10^8 independent transformants was obtained. Sequencing of 10 random clones revealed a nucleotide substitution rate of 1.3%.

Cloning, expression, and purification of receptor-binding domain. A gene encoding the S protein of the SARS-CoV Urbani strain (AY278741) was generously provided by S. Makino (UTMB-Galveston) and used to amplify the receptor-binding domain (RBD), consisting of amino acids 318 to 518. The RBD was cloned into pFastbac vector (Invitrogen) with the N-terminal honeybee melittin signal sequence (30) for secretion in insect cells, a C-terminal FLAG tag for screening, and an N-terminal 6-His tag for purification. Bacmid DNA was prepared and transfected into SF9 cells by using a Bac-Bac system (Invitrogen) according to the manufacturer's instructions to generate and amplify baculovirus particles, and the titers were determined by following the Bac-Bac protocol. High Five cells (Invitrogen) were cultured in insect Xpress medium (Cambrex, Walkersville, MD) supplemented with 10% fetal bovine serum (Sigma) and penicillin and streptomycin (Sigma) at 27°C as a monolayer. To produce the RBD, insect cells were seeded at a density of 10^6/ml in 250 ml of medium and infected at a multiplicity of infection of 5 with recombinant RBD baculovirus. Media were harvested after 90 h, and the culture supernatant was dialyzed against 1× IMAC (immobilized metal affinity chromatography) buffer (10 mM Tris-HCl, 0.5 M NaCl [pH 8.0]) at 4°C. Following dialysis, the culture supernatant containing the RBD was incubated with 1 ml of nickel-nitrilotriacetic acid (Ni-NTA) agarose (Qiagen, Hilden, Germany) for 2 h at 4°C. The mixture was then loaded onto a 5-ml column and washed with 10 column volumes of 1× IMAC buffer. Protein was eluted with 3 column volumes of 1× IMAC buffer with 300 mM imidazole. The protein eluate was further purified on a Superdex-200 (GE Healthcare) size exclusion column via fast protein liquid chromatography (FPLC). Protein samples were analyzed for purity on a 4 to 20% polyacrylamide gel (NuSep, Lawrenceville, GA) and stained with Coomassie blue.

Screening and selection of high-affinity scFv variants by APEx. *E. coli* strain Jude1 cells transformed with the 80R scFv library in the pAPEx1 vector were used to inoculate shake flasks containing 20 ml of Terrific broth (TB) medium (Difco, Sparks, MD) supplemented with chloramphenicol (Cm) at 35 μg/ml to an optical density at 600 nm (OD_{600}) of 0.1. Cells were grown at 37°C with shaking until the OD_{600} reached 0.5, at which point cultures were transferred to a 25°C shaker for 30 min. Protein synthesis was induced with isopropyl-β-D-thiogalactopyranoside (IPTG) to a final concentration of 1 mM, and incubation was continued for 3 h at 25°C with shaking. Two to three ml of cells equivalent to an OD_{600} of 10 were collected by centrifugation and resuspended in 350 μl of ice-cold Tris-sucrose (0.75 M sucrose and 0.1 M Tris-HCl [pH 8.0]) solution with 30 μl of 40 μg/ml lysozyme. An additional 700 μl of ice-cold 1 mM EDTA was added dropwise, and the mixture was incubated at 4°C on a rotary shaker for 15 min. A 50-μl portion of 0.5 M $MgCl_2$ was then added, and the mixture was incubated for another 10 min at 4°C on a rotary shaker. Cells were then gently pelleted, resuspended in 1 ml 1× PBS with purified RBD (100 nM for the first round), and incubated for 40 min at room temperature on a rotary shaker. Subsequently, the cells were pelleted again and resuspended with 1 ml 1× PBS with 200 nM phycoerythrin (PE)-conjugated anti-FLAG (Phycolink; Prozyme, San Leandro, CA) at room temperature for 40 min. After labeling, the cells were pelleted and resuspended in 1 ml 1× PBS and analyzed on a FACS Aria (BD Biosciences) flow cytometer using a 488-nm laser for excitation. The spheroplasts were gated based on forward-scatter and side-scatter parameters. Five percent of the most fluorescent cells were collected, and the sort population was

re-sorted immediately. scFv genes in the re-sort solution were amplified by PCR, cloned into the pAPEx1 vector, transformed into cells, and plated on agar plates. The resulting clones were then subjected to an additional three rounds of sorting as described above, except that decreasing concentrations of the RBD were used to increase the stringency of sorting as follows: 100 nM in the first round, 50 nM in the second, 25 nM in the third, and 20 nM in the final round.

After the fourth round of sorting via FACS, genes were rescued by PCR and cloned into pMopac16 (11) for soluble expression. For high-throughput off-rate screening based on dissociation rate constants, colonies were inoculated into a 96-well seed plate containing 200 μl of TB with 2% glucose and 200 μg/ml ampicillin per well. After overnight growth at 37°C with shaking, 20 μl of the culture from each well was used to inoculate fresh 96-well plates with the same growth medium. The seed plate was stored with 15% glycerol at −20°C for future use. After overnight growth at 37°C with shaking, cultures were pelleted by centrifugation at 4,500 rpm for 10 min. The medium was discarded; the cell pellets were resuspended in 200 μl of expression medium (TB with 200 μg/ml ampicillin and 1 mM IPTG) and then incubated at 25°C for 3 h. The cells were pelleted again by centrifugation at 4,500 rpm for 10 min, resuspended in 200 μl of lysis buffer (20% BugBuster HT-Novagen in HBS-EP buffer), and incubated with shaking at room temperature for 2 h. The lysates were centrifuged to precipitate the insoluble fraction, and the lysate supernatant was transferred to a 96-well multiscreen HTS filter plate (Millipore, Billerica, MA), set on a collection plate, and centrifuged for 10 min, and clarified filtrate was collected in a 96-well collection plate. The clarified filtrate was used for k_{off} determination by surface plasmon resonance (SPR) analysis using a BIAcore 3000 instrument (GE Healthcare, Uppsala, Sweden) as follows: purified RBD was first covalently immobilized in 10 mM sodium acetate (pH 5.9) on a CM5 sensor chip (carboxymethylated dextran matrix; GE Healthcare, Uppsala, Sweden) by using 1-ethyl-3-(3-dimethylaminopropyl) carbodiimide–*N*-hydroxysuccinimide chemistry to the level of 300 response units (RUs). Bovine serum albumin (BSA) was similarly coupled to the chip as an in-line subtraction standard. Kinetic analysis was performed in HBS-EP buffer (GE Healthcare, Uppsala, Sweden) at a flow rate of 25 μl/min at 25°C. Samples were injected over the immobilized RBD for 2 min followed by a 5-min dissociation phase. The surface was regenerated by injection of 10 μl of 4 M $MgCl_2$ at a 50 μl/min flow rate. Dissociation kinetics were calculated using BIAevaluation software, and clones with the lowest off rates compared to that of 80R were selected for further analysis.

Shuffling and random mutagenesis of isolated clones for additional screening. The four highest-affinity scFv genes isolated from the off-rate analysis described above, along with the 80R scFv gene, were chosen for DNA shuffling. The four isolated genes were first amplified individually by PCR, and the DNA products were pooled with a 4-fold molar excess of 80R scFv and then digested with 0.125 U of DNase I (Roche, Germany) per 3 μg of DNA at room temperature for 30 min. The reaction was stopped by heat inactivation at 80°C for 10 min, and DNase I digest fragments of 50 to 100 bp were gel purified using a QIAEX II (Qiagen) gel extraction kit. The DNA fragments were reassembled by PCR for a few rounds without primers; then full-length DNA was amplified using externally flanking primers encoding SfiI sites. DNA was separated by agarose gel electrophoresis, and a band ~750 bp in length was excised, gel purified using the Qiagen gel extraction kit (Qiagen), digested with SfiI, and then ligated to SfiI-digested pAPEx1 vector. Following electroporation, 5.4×10^7 transformants were obtained, and DNA sequencing of 10 clones selected at random revealed the presence of recombination events as expected. PCR product after the assembly was also used as a template for error-prone PCR as described above, and the DNA product from that reaction was cloned into pAPEx1 vector to generate a library of 1.5×10^7 transformants with a nucleotide substitution rate of 0.5%.

The shuffled library and the error-prone library were pooled and subjected to three rounds of FACS screening as described above. The concentration of the RBD used for labeling was reduced in successive rounds as follows: 20 nM for the first round, 10 nM for the second round, and 5 nM for the final round. After the final round of sorting, scFv genes were PCR amplified and subcloned into pMopac16. Subsequently, 96 colonies were inoculated for high-throughput screening, cell lysates were prepared, and dissociation rate constants were measured using SPR as described above.

Expression and purification of single-chain antibody fragments (scAbs). Antibody fragments were expressed as scAbs by inserting the scFv genes into pMopac16 vector, a pAK400 derivative in which the scFv is fused in frame to a C-terminal human kappa light-chain constant domain.

Antibody fragments were expressed in *E. coli* Jude1 (DH10BF::Tn*10*) (11). Individual colonies were inoculated into 50 ml TB medium with 200 μg/ml ampicillin and 2% glucose and were grown overnight at 37°C. Overnight cultures were used to inoculate 500 ml of TB medium with 200 μg/ml ampicillin, and the cells were grown at 37°C for 3 h. Cultures were transferred to 25°C for 30 min, and protein expression was induced with 1 mM IPTG. After 4 h of incubation at 25°C, cells were collected by centrifugation, and protein was purified from the osmotic shock fraction (11). Briefly, cells were resuspended in 12 ml of ice-cold Tris-sucrose solution (0.75 M sucrose, 100 mM Tris [pH 8]) with the addition of 1 ml of 30 μg/ml lysozyme in Tris-sucrose buffer. Cells were gently mixed for 10 min at 4°C, and 24 ml of 1 mM EDTA was added dropwise and allowed to mix for an additional 20 min at 4°C. A 1.7-ml portion of 0.5 M $MgCl_2$ was added, and the mixture was incubated further for 10 min. The samples were centrifuged at 12,000 rpm for 15 min, and the resulting supernatant was dialyzed against 1× IMAC buffer (10 mM Tris-HCl, 0.5 M NaCl [pH 8.0]). ScAbs were purified from the supernatant by IMAC using Ni-NTA agarose according to the manufacturer's protocol (Qiagen, Hilden, Germany), followed by size exclusion FPLC on Superdex 200 (GE Healthcare) as described above. The purity of isolated scAb was verified by gel electrophoresis on a 4 to 20% SDS-PAGE gel (NuSep, Lawrenceville, GA) stained with Coomassie blue.

To remove the endotoxin from the purified scAbs for *in vitro* neutralization assays, the purified protein samples were passed three times through Detoxi-gel endotoxin removal columns (Pierce, Rockford, IL) according to the manufacturer's instructions. The endotoxin levels in the samples were measured by the limulus amebocyte lysate (LAL) assay (Associates of Cape Cod, East Falmouth, MA) as described by the manufacturer.

BIAcore analysis for affinity measurement. The purified RBD was immobilized on aCM5 chip as described above, and BSA was used as in-line subtraction. Kinetic analysis was performed in HBS-EP buffer at a flow rate of 50 μl/min at 25°C. The affinity of the FPLC-purified scAbs was analyzed by injecting the samples over the chip for 1 min for the association phase followed by 10 min dissociation. Five different concentrations of antibodies from 9 nM to 36 nM were analyzed in duplicate, along with a blank as a reference. The surface regeneration was performed with a 12-s injection of 4 M $MgCl_2$. Binding kinetics were calculated using BIA evaluation software (GE Healthcare, Uppsala, Sweden). Calculated fits were based on the Langmuir 1:1 model, with χ^2 values below 1.

Isolation of escape mutants under neutralizing antibody selective pressure. icUrbani (1×10^6 PFU) was incubated with 20 μg of a neutralizing scAb (RSK, SK4, or 80R) in a 200-μl volume for 30 min and then inoculated onto VeroE6 cells in the presence of the respective scAb antibody fragment at a concentration of 20 μg/ml. The development of cytopathic effect (CPE) was monitored over 72 h, and progeny viruses were harvested. Antibody treatment was repeated two additional times, and more rapid CPE was noted with each passage. The viruses from passage 4 were plaque purified in the presence of antibody; neutralization-resistant viruses were stored at −80°C, and titers were determined on VeroE6 cells as described above. The S glycoprotein genes from four individual plaques for each experiment were sequenced, and the neutralization titers between wild type and antibody-resistant viruses were determined as described below.

In the experiment described above, the SK4 scAb resulted in the ex-

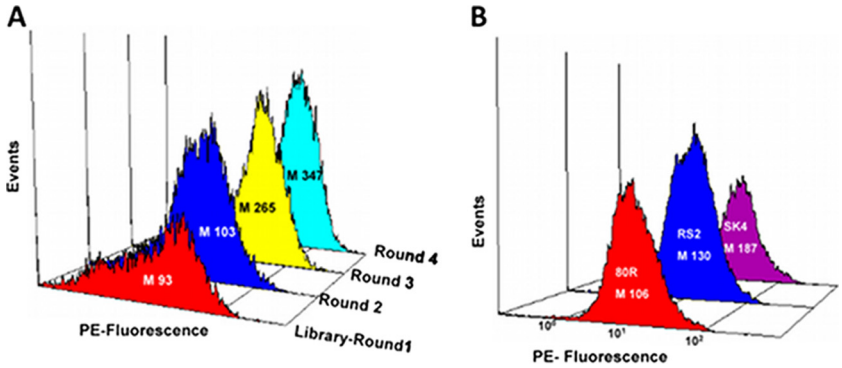

FIG 1 Comparison of fluorescence histograms. *E. coli* spheroplasts were labeled with 20 nM RBD, and binding was detected with 200 nM anti-FLAG PE. (A) Mean fluorescence intensity (M) of *E. coli* spheroplast clones recovered after three successive rounds of sorting compared to a library of random mutants of the 80R scFv. (B) Mean fluorescence intensity (M) of *E. coli* cells expressing the RS2 and SK4 scFvs compared to 80R scFv.

tinction of parent viruses on three separate occasions. To increase the probability of escape mutant evolution, we incubated 1×10^6 PFU of icUrbani with decreasing concentrations of SK4 ScAb antibody fragment (15, 10, 5, and 1 μg) for 30 min and then infected cultures in the presence of 5 μg/ml SK4 antibody. Depending on treatment conditions, cytopathology either was evident within 48 h (5- and 1-μg doses) or was minimal after 4 days (15 and 10 μg). Low-dose-SK4-treated progeny viruses (1- and 5-μg doses) were treated with 5 μg of SK4 for two passages and then selected with two additional treatments of 10- and 15-μg doses each, resulting in highly antibody-resistant viruses that produced extensive CPE in cultures within 24 to 36 h. High-dose-treated stocks were passaged once in the absence of antibody (pass 2) to restore virus titers and then reselected twice in the presence of 5 μg antibody. Two final treatments of 10 and 15 μg of SK4 antibody resulted in highly resistant populations that rapidly produced CPE in culture. Two to four plaques were isolated from each treatment regimen (9 plaques total) in the presence of 20 μg SK4 antibody, and the S glycoprotein gene was sequenced.

Plaque reduction neutralization test (PRNT). Each scAb in the panel (80R, RSK, RS2, and SK4) was serially diluted 1:2 in PBS starting at 30 μg/ml. Wild-type icUrbani, icGD03-MA, and icHC/SZ/61/03 were diluted, and approximately 100 PFU of each was added to the scAb dilution series for 30 min at 37°C. The percentage neutralization was calculated as [100 − (number of plaques with antibody/number of plaques without antibody)] × 100. For 50% plaque reduction neutralization titers ($PRNT_{50}$s) of single-substitution variants, the viruses were diluted to 100 PFU and added to 2-fold serial dilutions of SK4 starting at 5 μg/ml. The single-substitution variants are escape mutants developed against monoclonal antibodies, as previously described (L443R and T332I [21] and D480G [26]) or as described above (Y436H, Y442S, and N479I).

RESULTS

Generation of high-affinity variants of the 80R scFv antibody. The RBD fused to a C-terminal FLAG peptide epitope (RBD-FLAG) was produced in High Five insect cells, with a yield of approximately 1.2 mg/liter. RBD-FLAG was purified to >95% homogeneity and was shown to bind to the 80R scAb (an scFv fragment fused to a human Cκ chain for improved expression and stability) with a dissociation constant in the nanomolar range, consistent with earlier reports (27).

The 80R scFv library was expressed as a fusion to the signal peptide and the first 6 amino acids of NlpA using the pAPEx1 vector. The short NlpA fusion anchors the scFv on the outer side of the *E. coli* inner membrane (9). Following spheroplast formation, a limiting amount of labeled antigen (RBD-FLAG) was added, followed by the addition of anti-FLAG PE; then screening by FACS led to enrichment in higher-affinity variants. Around 5% of the spheroplasts with the highest fluorescence were collected and re-sorted. The scFv genes from the sorted cells were rescued by PCR amplification and cloned back into pAPEx1. After three additional rounds of sorting with decreasing concentrations of RBD-FLAG from 100 nM to 20 nM (Fig. 1A), scFv genes were rescued by PCR and expressed as soluble scAb antibody fragments for biochemical analysis.

A total of 88 randomly picked colonies from round 4, as well as 8 colonies of cells expressing 80R scAb as controls, were grown in a 96-well plate. Following chemical lysis, the k_{off} rate constants of the scAb proteins in the lysates were rank ordered by surface plasmon resonance (SPR) analysis. Four scAb antibody fragments displaying the lowest antigen dissociation rates were expressed and purified to near homogeneity by IMAC followed by gel filtration FPLC. SPR analysis revealed that all the isolated scAbs exhibit significantly lower K_D values for RBD binding than the 80R antibody fragment and that the improvements in K_D values arose primarily because of lower k_{off} values (9). The K_D values of the scAb variants ranged from 0.86 nM to 0.05 nM, with the highest-affinity clone, RS2, exhibiting a k_{off} of 1.34×10^{-4} s^{-1} (Table 1). This represents a >200-fold improvement in affinity relative to 80R (K_D = 10.5 nM).

Sequence analysis of the isolated clones revealed a variety of mutations distributed over the entire length of the scFv gene (5 to 8 amino acid substitutions per gene). Most of the amino acid substitutions were present in the framework regions, with only one consensus mutation, S167N, being observed in the CDR1 light chain of all four clones (data not shown). S167 is located at the interface of the cocrystal of the 80R-RBD complex (12), indi-

TABLE 1 Equilibrium dissociation constant values (K_Ds) of scAbs with RBD, as measured by SPR analysis

Clone[a]	k_a (1/Ms)	k_d (1/s)	K_D (nM)	Fold difference
80R	$1.50 \times 10^6 \pm 0.06$	$1.60 \times 10^{-3} \pm 0.001$	10.5 ± 0.09	1
RS2	$2.69 \times 10^6 \pm 0.12$	$1.34 \times 10^{-4} \pm 0.43$	0.05 ± 0.01	210
SK4	$2.03 \times 10^6 \pm 0.8$	$6.91 \times 10^{-5} \pm 0.9$	0.037 ± 0.01	270
RSK	$1.73 \times 10^5 \pm 0.009$	$1.91 \times 10^{-4} \pm 0.4$	0.11 ± 0.03	95

[a] 80R, parental clone; RS2, isolated from round 1 screening; SK4, isolated from round 2 screening; RSK, 80R with S167N, N57S, and S188N mutations.

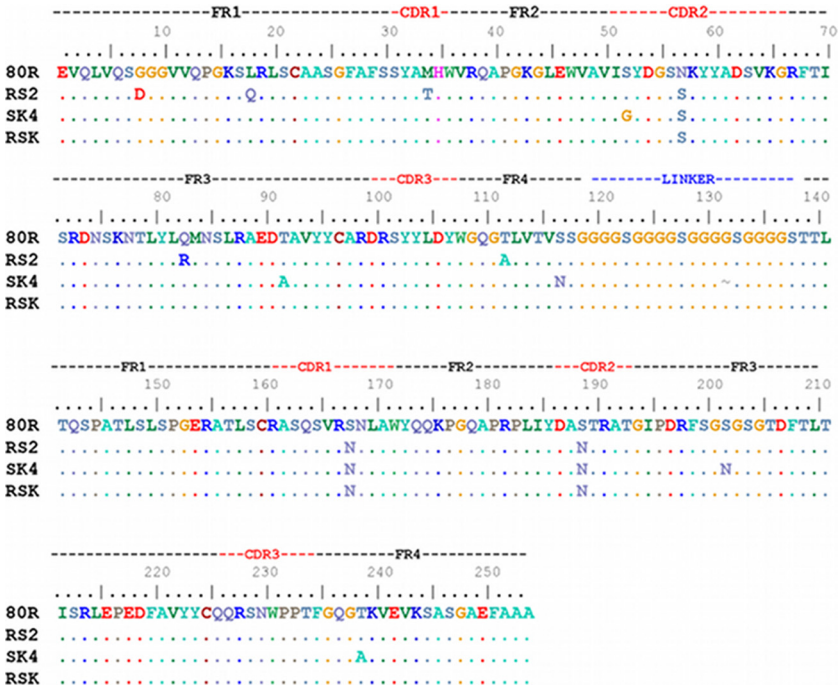

FIG 2 Sequence comparison of the engineered, high-affinity variants RS2, SK4, and RSK with parental 80R scFv. Single-chain antibody fragments were constructed in the variable heavy (VH)–linker–variable light (VL) orientation.

cating its possible involvement in RBD binding. The significance of this mutation was recently highlighted by the studies of Sui and coworkers (26), who reported that an S167N substitution in 80R is important for broad neutralization of SARS-CoV icUrbani strain escape variants containing a D480A or D480G mutation.

The four high-affinity clones described above, together with the parental antibody 80R, were subjected to *in vitro* recombination by DNA shuffling followed by random mutagenesis using error-prone PCR. In DNA shuffling reactions, the 80R scFv was used at a 4-fold molar excess in order to reduce the number of neutral mutations. Two libraries were constructed, a shuffled library comprising 5.4×10^7 transformants and an error-prone library of 1.5×10^7 transformants. The libraries were pooled and screened by APEx with antigen concentrations starting at 20 nM in the first round and decreasing to 5 nM in the third and final round. The antigen dissociation rate constants for 80 clones from the third round were analyzed by SPR analysis, and two clones with lower off rates were identified. SPR analysis of the purified monomeric scAb protein from the highest-affinity clone, SK4, yielded a K_D value of 37 pM and a k_{off} of 6.91×10^{-5} s^{-1} (Fig. 1B; Table 1). Overall, the SK4 antibody fragment displayed 270-fold higher affinity than 80R and contained eight amino acid substitutions, including three mutations in common with RS2: N57S, S167N, and S188N (Fig. 2).

To determine the role of the N57S, S167N, and S188N amino acid substitutions in affinity enhancement, the respective mutations were introduced into the 80R scAb by site-directed mutagenesis to construct a variant referred to as RSK (Fig. 2). SPR analysis of the RSK antibody fragment revealed a K_D value of 110 pM, indicating that some or all of these three amino acid substitutions confer affinity improvement (Fig. 2; Table 1).

SARS CoV neutralization and escape. To evaluate the neutralizing ability of the purified 80R, SK4, and RSK scAbs, we conducted plaque reduction neutralization titer assays with each of the scAbs against SARS-CoV (icUrbani). As expected, the neutralization potencies of the antibodies increased according to affinity. Compared to 80R (IC_{50}, 0.722 μg/ml), both RSK and SK4 exhibited 10-fold-greater neutralization (IC_{50}, 0.069 μg/ml and 0.059 μg/ml, respectively) (Fig. 3). For antibodies 80R and RSK, *in vitro*

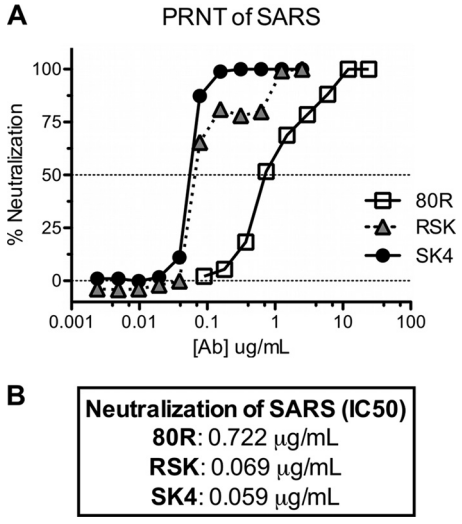

FIG 3 Neutralization activity of the SK4 and RSK scAbs in comparison to 80R. Neutralization activity was tested by plaque reduction assay against icUrbani. Approximately 100 PFU of icUrbani was incubated with the scAb dilution series. The percentage neutralization was calculated as [100 − (number of plaques with antibody/number of plaques without antibody)] × 100.

TABLE 2 Amino acid changes in the RBD of spike protein found in the neutralization escape mutants

ScAb	Mutation(s)	No. of clones with mutation/ total sequenced
80R	D480A	3/4
	D480Y	1/4
SK4	N479I + D480Y	9/9
RSK	D480Y	3/4
	Y436H	1/4

TABLE 3 Amino acid differences in the RBD of the spike protein

Strain	Amino acid at position:						
	344	360	436	472	479	480	487
Urbani (human 02/03)	K	F	Y	L	N	D	T
HC/SZ/61/03 (civet)	R	S	Y	P	R	G	S
GD03MA (mouse-adapted human 03/04)	R	S	H	P	N	G	S

neutralization escape mutants of the icUrbani strain emerged after three passages in cell culture, and four plaques for each antibody were picked for sequence analysis. Three of the four 80R escape mutants carried a mutation from aspartic acid to alanine at position 480 (D480A), and one had a mutation of aspartic acid to tyrosine (D480Y), replicating the D480 residue identified by previous selection with the full IgG version of this antibody (26, 28). In the case of the RSK antibody, three of the four escape variants had the D480Y mutation and one had a Y436H mutation (Table 2).

Importantly, the SK4 antibody exhibited very high neutralizing potency, and 20 μg was sufficient to completely extinguish 1×10^6 PFU of the parent virus, yielding no escape variants. Therefore, the initial concentration of SK4 scAb was decreased to reduce the selective pressure and was incrementally increased over multiple viral passages. A total of nine plaques were isolated from the final selection with 20 μg SK4 and sequenced.

All nine of the isolated escape mutants contained two mutations: N479I and D480Y (Table 2). Both D480 and N479 have been found to be highly adapted RBD residues that allow specific binding to hACE2, and mutations at these positions decrease their affinity for hACE2 and hence infectivity (37). D480 has been shown to have a critical role in the binding of the parental antibody 80R to the RBD (12, 28), and substitution to a tyrosine has been shown not to affect the binding of the RBD (and therefore the virus) to the human ACE2 receptor (34). The mutation N479I had been found in bananin-resistant virus, and this position is found to correspond to a highly variable site in the RBD (33).

Cross neutralization studies with mutant viruses encoding either D480A or D480Y, which mediated escape from 80R and its derivatives, were performed with all three antibodies (Fig. 4). Importantly, SK4 successfully neutralized both escape mutants, suggesting an enhanced role for high affinity in overcoming the effect of D480 substitutions. We note, however, that none of the scAbs could neutralize the civet strain icHC/SZ/61/03 or the mouse-adapted variant of the human 03/04 strain, icGD03MA; the latter strain carries a Y436H mutation associated with increased mACE2 receptor usage (1, 19) (data not shown). The spike proteins of GD03 MA and HC/SZ/61/03 each differ from that of the icUrbani strain at six other amino acid positions within the RBD (Table 3), and evidently, at least some of these are critical for antibody binding.

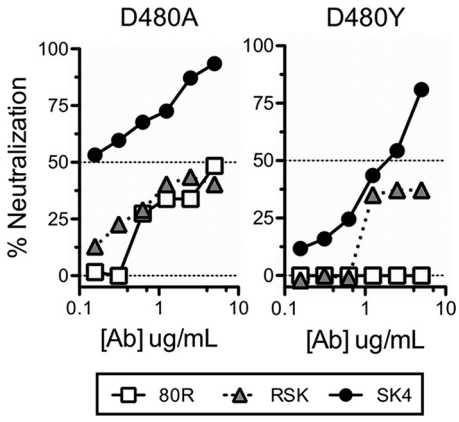

FIG 4 Cross neutralization studies of high-affinity scAbs with escape mutants with the D480A and D480Y mutations.

To further assess the breadth of SK4 neutralization, we tested SK4 neutralization against several viruses that emerged as escape variants to other monoclonal antibodies reported earlier (21, 26). These viruses contained single substitutions in the RBD, both within and outside the 80R/SK4 interface. Two escape variants, L443R and T332I, were developed under selection with the broadly neutralizing antibodies s230.15 and s109.8, respectively (21). Residue 443 is a contact interface site with ACE2 but not with 80R, while residue 332 does not directly interface with either 80R or ACE2. The escape variants Y436H, Y442S, N479I (data not shown), and D480G emerged following selection with 80R derivative antibodies and contain substitutions that interface with 80R and, except for D480G, also interface with the ACE2 receptor (12).

SK4 was capable of neutralizing all six of these antibody escape variants. Three of the escape variants, namely, Y436H, Y442S, and T332I, were neutralized with an efficacy comparable to that observed with icUrbani (IC_{50}s of 0.049 μg/ml, 0.039 μg/ml, and 0.109 μg/ml, respectively, compared to 0.059 μg/ml for icSARS) (Fig. 5). Importantly, SK4 neutralized three other escape variants, with IC_{50}s lower than the IC_{50} displayed by 80R for icUrbani [0.234 μg/ml (L443R), 0.432 μg/ml (N479I), and 0.542 μg/ml (D480G), compared to an IC_{50} of 0.722 μg/ml for 80R with icUrbani]. Thus, viruses containing amino acid substitutions at either N479 or D480, which when combined mediated escape from SK4, were neutralized with a lower IC_{50} than that of 80R for icUrbani.

DISCUSSION

SARS was the first new major infectious disease to challenge the world population in the 21st century (42). Though the number of deaths resulting from the disease was small in comparison to previous pandemics, such as those caused by plague and influenza, the widespread fear and resulting travel restrictions resulted in a global economic cost estimated at 59 billion dollars (42). Since the identification of the virus, significant research effort has been focused on the development of neutralizing antibodies for use in both prophylaxis and therapy. Antibodies targeting the RBD region of the viral spike S protein have been shown to be protective

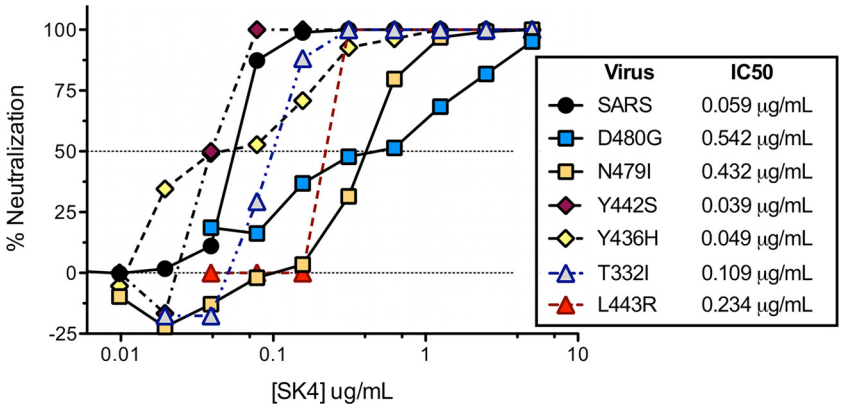

FIG 5 SK4 neutralization of escape variants. Neutralization activity of SK4 was tested against escape variants, and the IC_{50}s were compared to that of icUrbani.

in both *in vitro* and in the mouse challenge model by blocking the viral attachment to the host cell receptor (27, 28, 44). However, the SARS-CoV S protein is subject to antigenic drift that has been documented both in clinical isolates and in escape variants identified from *in vitro* antibody neutralization experiments. The use of antibody cocktails consisting of multiple monoclonal antibodies for preventing the evolution of escape mutants is generally impractical as a therapeutic approach, due to both high cost and long development times. Alternatively, we show here that antibody engineering strategies can be employed to induce broader neutralization breadth and/or higher potency based on affinity improvement. Earlier, Sui and coworkers developed broadly neutralizing antibodies by selecting for variants of 80R that could recognize the RBD D480A or D480G escape mutants as well as icUrbani (26) by relying on *a priori* knowledge of naturally occurring escape mutations in the RBD.

Here we used random mutagenesis and screening using the bacterial display technique APEx (9) to engineer a series of 80R scFv variants with increased antigen affinity. Variants with dissociation constants (K_Ds) of 0.86 nM, 50 pM, and 37 pM were obtained, representing a >270-fold improvement compared to the parent 80R antibody (K_D of 10.5 nM on a BIAcore 3000 instrument) (Table 1). Only one consensus mutation, S167N, in CDR1 of the light chain, was observed in all of the affinity-improved variants (Fig. 2). Interestingly, S167N was also identified by Sui and coworkers in all 80R variants selected to bind to RBD(D480A) or RBD(D480G) and showing broader neutralization (26). However, the S167N-containing variants in that study displayed only a modest (3-fold) increase in antigen affinity. A structure-based prediction of the interaction between these antibody variants with RBD suggests that in wild-type 80R, S167 is proximal to D480 of the RBD and likely interacts with D480, perhaps through a hydrogen-bonded water molecule. The bulkier S167N mutation appears to preclude the presence of any bound water molecule for steric reasons. The slightly bulkier Asn likely moves the hydrogen binding potential away from D480, allowing a higher-affinity electrostatic interaction between D480 and R166 (Fig. 6). Two more mutations, N57S and S188N, were conserved in the high-affinity variants RS2 and SK4 (Fig. 2). When S167N, N57S, and S188N were introduced into 80R, the affinity of the resulting antibody, RSK, increased nearly 100-fold, suggesting that the combination of all three mutations allows a much better fit to the RBD interface. In addition to the enhanced binding to D480, the S167N substitution may also mediate direct interactions with N479. Finally, molecular modeling indicates that the N57S mutation removes interactions with R426 and T485 of the RBD, suggesting that these mutations work in concert to allow a better fit to the RBD interface. (Fig. 6).

Our *in vitro* neutralization studies have provided compelling evidence that an antibody engineered with higher affinity can lead to more potent and broader virus neutralization. In particular, the SK4 and RSK antibody fragments exhibited markedly higher neutralization potency against the icUrbani strain (Fig. 3) than 80R. In addition, cross neutralization studies revealed that SK4 successfully neutralized the 80R escape mutants containing either the D480A or D480Y mutation in the RBD. These mutations probably eliminate the electrostatic interaction between D480 of the RBD and R166 of SK4. However, the polar interactions of N167, N188, and N201 of SK4 with N473, Y442, and N479 of the RBD would probably be sufficient to preserve strong binding between SK4 and these mutants (Fig. 6).

Individually, the substitutions N479I and D480G each cause a shift in neutralization that is nonetheless insufficient to escape SK4, reinforcing the necessity of double substitutions to escape the high-affinity neutralization by SK4. Additional substitutions either selected by 80R-derived antibodies or derived independently of 80R antibodies are also incapable of providing escape from SK4. It is worth noting, however, that while SK4 is capable of neutralizing each of the single-substitution spike variants we tested, it is unable to neutralize the more divergent spikes, i.e., those containing variants in six or seven positions relative to the icUrbani strain. This suggests that high-affinity neutralizing antibodies like SK4 would provide excellent resistance to escape and would be best paired with a broadly neutralizing antibody for a highly effective therapeutic cocktail.

Just as important as neutralization breadth, higher affinity appeared to suppress the formation of viral escape mutants. At a concentration of 80R that readily gave rise to escape mutants, incubation with the highest-affinity antibody, SK4, led to no CPE or viral plaques after multiple attempts. In order to further understand the potential role affinity might play during simulated infection, the anti-RBD antibodies were intentionally used at subneutralizing concentrations in an effort to generate viral escape mutants. Sequencing revealed that the most common RBD mutation observed in the escape mutants generated by all antibodies was D480Y. For SK4, the highest-affinity antibody in the study,

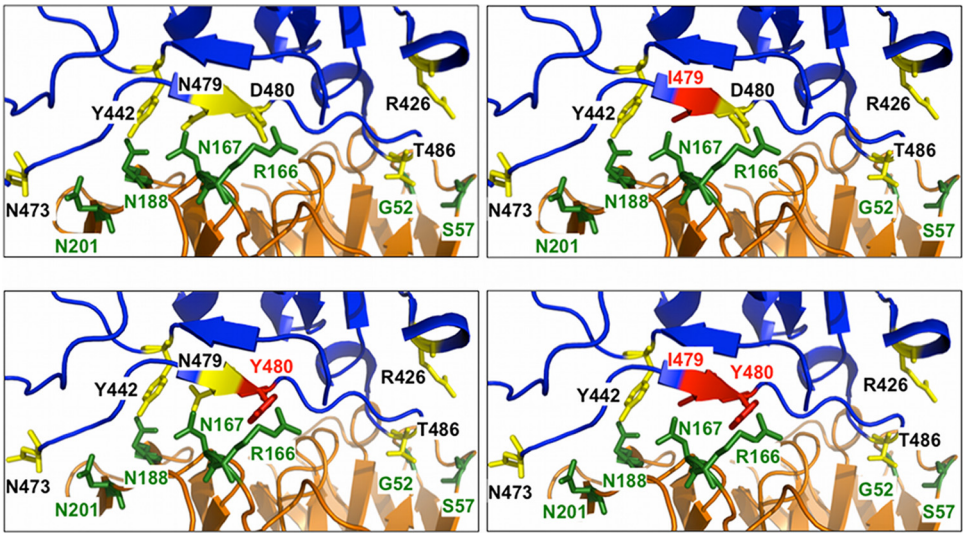

FIG 6 Effect of escape mutations on SK4. (Top left) SK4 interacts robustly with RBD via polar interactions involving N167, N188, and N201 of SK4 with N473, Y442, and N479 of the RBD. An electrostatic interaction between D480 of the RBD and R166 of SK4 also contributes to robust binding. (Top right) An escape mutant with N479I would likely still interact strongly with SK4. While I479 would not participate in polar interactions with N167, N188, and N201, the electrostatic interaction between D480 of the RBD and R166 of SK4 would be sufficient to allow strong binding of SK4 to the RBD mutant. (Bottom left) A mutant with a D480Y change would knock out the electrostatic interaction between D480 of the RBD and R166 of SK4, but the polar interactions of N167, N188, and N201 of SK4 with N473, Y442, and N479 of the RBD would be sufficient to preserve strong binding between SK4 and this mutant. (Bottom right) Only the double mutation N479I plus D480Y would allow escape from SK4 binding, as this mutation would disrupt two robust binding residues. Residues 430 to 435 and 469 to 472 of the RBD have been removed to allow better visualization of the structures. Blue, RBD; orange, SK4; yellow, RBD-interacting residues; green, SK4-interacting residues; red, mutation sites 479I and 480Y.

escape mutants could be generated only when the concentration of antibody was reduced further, and it required two mutations in the RBD: N479I and D480Y. The accumulation of two mutations for escape from the action of the neutralizing antibody would of course be expected to be a much more rare event, and thus the incidence of such escape variants in a therapeutic setting would likely be low. However, we do note that even SK4 failed to neutralize SARS-CoV HC/SZ/61/03 and GD03MA, presumably because the RBD in these strains contains multiple mutations that drastically alter the character of the binding epitope (Table 3).

All of the high-affinity 80R variants used in this study were isolated after just one round of random mutagenesis followed by DNA shuffling using bacterial display by APEx. This approach should be equally applicable to new and evolving strains and could be employed for the generation of SK4 variants that can also recognize civet and human strains that presently are not neutralized by this antibody.

A number of studies have established that antibody affinity plays a critical role in toxin or virus neutralization potency *in vivo* (17, 36). It is thought that during the germinal center reaction in the immune system, kinetic considerations impose a limit on the affinity during B-lymphocyte selection, keeping K_D values in the range of 1 nM (5). Thus, antibodies displaying higher affinities, with K_Ds in the picomolar range or lower (4), typically must be generated using *in vitro* mutagenesis and screening techniques.

In a recent study, Zhang et al. used a sequential antigen panning (SAP) method and successfully isolated broadly cross-reactive antibodies with two- to threefold lower IC_{50}s than the parent HIV-1-neutralizing antibody scFv X5 (41). Upon further characterization, they found that the highly potent m9 antibody not only exhibited broad neutralizing activity but also suppressed the generation of escape mutants upon immune selection (40). Additional studies on broadly neutralizing antibodies to HIV from memory B cells also suggest that affinity has an important role in breadth and potency of neutralization (23, 31).

However, one needs to proceed with caution. In the case of motavizumab, a high-affinity variant of palivizumab (Synagis), a higher incidence of immunogenicity was seen in phase III clinical trials that led to discontinuation of its development as a therapeutic agent (2, 31, 43). Collectively, our results together with evidence from earlier studies support the notion that very high-affinity neutralizing antibodies may be particularly useful in a therapeutic setting and suppress the emergence of escape variants.

ACKNOWLEDGMENTS

This work was supported by the Texas Higher Education Coordinating Board, Norman Hackerman Advanced Research Program (grant 003658-0066-2009), and by the National Institutes of Health (award 1 U01AI078008). R.B. was supported by the National Institutes of Health (R0 1AI085524), and M.B. was supported by the University of North Carolina—Chapel Hill Medical Science Training Program (T32GM008719).

We thank S. Makino, UTMB Galveston, for assistance in some of the early studies related to this work and Sara Sawyer for comments on the manuscript.

REFERENCES

1. **Becker MM, et al.** 2008. Synthetic recombinant bat SARS-like coronavirus is infectious in cultured cells and in mice. Proc. Natl. Acad. Sci. U. S. A. **105**:19944–19949.
2. **Cingoz, O.** 2009. Motavizumab. MAbs **1**:439–442.
3. **Du L, et al.** 2009. The spike protein of SARS-CoV—a target for vaccine and therapeutic development. Nat. Rev. Microbiol. **7**:226–236.
4. **Foote J, Eisen HN.** 2000. Breaking the affinity ceiling for antibodies and T cell receptors. Proc. Natl. Acad. Sci. U. S. A. **97**:10679–10681.
5. **Foote J, Winter G.** 1992. Antibody framework residues affecting the conformation of the hypervariable loops. J. Mol. Biol. **224**:487–499.

6. **Fromant M, Blanquet S, Plateau P.** 1995. Direct random mutagenesis of gene-sized DNA fragments using polymerase chain reaction. Anal. Biochem. **224**:347–353.
7. **Greenough TC, et al.** 2005. Development and characterization of a severe acute respiratory syndrome-associated coronavirus-neutralizing human monoclonal antibody that provides effective immunoprophylaxis in mice. J. Infect. Dis. **191**:507–514.
8. **Griswold KE, et al.** 2005. Evolution of highly active enzymes by homology-independent recombination. Proc. Natl. Acad. Sci. U. S. A. **102**: 10082–10087.
9. **Harvey BR, et al.** 2004. Anchored periplasmic expression, a versatile technology for the isolation of high-affinity antibodies from Escherichia coli-expressed libraries. Proc. Natl. Acad. Sci. U. S. A. **101**:9193–9198.
10. **Hayhurst A.** 2000. Improved expression characteristics of single-chain Fv fragments when fused downstream of the *Escherichia coli* maltose-binding protein or upstream of a single immunoglobulin-constant domain. Protein Expr. Purif. **18**:1–10.
11. **Hayhurst A, et al.** 2003. Isolation and expression of recombinant antibody fragments to the biological warfare pathogen Brucella melitensis. J. Immunol. Methods **276**:185–196.
12. **Hwang WC, et al.** 2006. Structural basis of neutralization by a human anti-severe acute respiratory syndrome spike protein antibody, 80R. J. Biol. Chem. **281**:34610–34616.
13. **Li F, Li W, Farzan M, Harrison SC.** 2005. Structure of SARS coronavirus spike receptor-binding domain complexed with receptor. Science **309**: 1864–1868.
14. **Li Y, Lipschultz CA, Mohan S, Smith-Gill SJ.** 2001. Mutations of an epitope hot-spot residue alter rate limiting steps of antigen-antibody protein-protein associations. Biochemistry **40**:2011–2022.
15. **Liang G, et al.** 2004. Laboratory diagnosis of four recent sporadic cases of community-acquired SARS, Guangdong Province, China. Emerg. Infect. Dis. **10**:1774–1781.
16. **Marra MA, et al.** 2003. The Genome sequence of the SARS-associated coronavirus. Science **300**:1399–1404.
17. **Maynard JA, et al.** 2002. Protection against anthrax toxin by recombinant antibody fragments correlates with antigen affinity. Nat. Biotechnol. **20**: 597–601.
18. **Nie Y, et al.** 2004. Neutralizing antibodies in patients with severe acute respiratory syndrome-associated coronavirus infection. J. Infect. Dis. **190**: 1119–1126.
19. **Roberts A, et al.** 2007. A mouse-adapted SARS-coronavirus causes disease and mortality in BALB/c mice. PLoS Pathog. **3**:e5. doi:10.1371/journal.ppat.0030005.
20. **Rockx B, et al.** 2008. Structural basis for potent cross-neutralizing human monoclonal antibody protection against lethal human and zoonotic severe acute respiratory syndrome coronavirus challenge. J. Virol. **82**:3220–3235.
21. **Rockx B, et al.** 2010. Escape from human monoclonal antibody neutralization affects in vitro and in vivo fitness of severe acute respiratory syndrome coronavirus. J. Infect. Dis. **201**:946–955.
22. **Rockx B, et al.** 2007. Synthetic reconstruction of zoonotic and early human severe acute respiratory syndrome coronavirus isolates that produce fatal disease in aged mice. J. Virol. **81**:7410–7423.
23. **Scheid JF, et al.** 2009. Broad diversity of neutralizing antibodies isolated from memory B cells in HIV-infected individuals. Nature **458**:636–640.
24. **Sheahan T, et al.** 2011. Successful vaccination strategies that protect aged mice from lethal challenge from influenza virus and heterologous severe acute respiratory syndrome coronavirus. J. Virol. **85**:217–230.
25. **Stemmer WP, Crameri A, Ha KD, Brennan TM, Heyneker HL.** 1995. Single-step assembly of a gene and entire plasmid from large numbers of oligodeoxyribonucleotides. Gene **164**:49–53.
26. **Sui J, et al.** 2008. Broadening of neutralization activity to directly block a dominant antibody-driven SARS-coronavirus evolution pathway. PLoS Pathog. **4**:e1000197. doi:10.1371/journal.ppat.1000197.
27. **Sui J, et al.** 2004. Potent neutralization of severe acute respiratory syndrome (SARS) coronavirus by a human mAb to S1 protein that blocks receptor association. Proc. Natl. Acad. Sci. U. S. A. **101**:2536–2541.
28. **Sui J, et al.** 2005. Evaluation of human monoclonal antibody 80R for immunoprophylaxis of severe acute respiratory syndrome by an animal study, epitope mapping, and analysis of spike variants. J. Virol. **79**:5900–5906.
29. **ter Meulen J, et al.** 2006. Human monoclonal antibody combination against SARS coronavirus: synergy and coverage of escape mutants. PLoS Med. **3**:e237. doi:10.1371/journal.pmed.0030237.
30. **Tessier DC, Thomas DY, Khouri HE, Laliberte F, Vernet T.** 1991. Enhanced secretion from insect cells of a foreign protein fused to the honeybee melittin signal peptide. Gene **98**:177–183.
31. **Toran JL, et al.** 2001. Improvement in affinity and HIV-1 neutralization by somatic mutation in the heavy chain first complementarity-determining region of antibodies triggered by HIV-1 infection. Eur. J. Immunol. **31**:128–137.
32. **Traggiai E, et al.** 2004. An efficient method to make human monoclonal antibodies from memory B cells: potent neutralization of SARS coronavirus. Nat. Med. **10**:871–875.
33. **Wang Z, et al.** 2011. On the mechanisms of bananin activity against severe acute respiratory syndrome coronavirus. FEBS J. **278**:383–389.
34. **Wong SK, Li W, Moore MJ, Choe H, Farzan M.** 2004. A 193-amino acid fragment of the SARS coronavirus S protein efficiently binds angiotensin-converting enzyme 2. J. Biol. Chem. **279**:3197–3201.
35. **Wu H, et al.** 2007. Development of motavizumab, an ultra-potent antibody for the prevention of respiratory syncytial virus infection in the upper and lower respiratory tract. J. Mol. Biol. **368**:652–665.
36. **Wu H, et al.** 2005. Ultra-potent antibodies against respiratory syncytial virus: effects of binding kinetics and binding valence on viral neutralization. J. Mol. Biol. **350**:126–144.
37. **Wu K, Peng G, Wilken M, Geraghty RJ, Li F.** 2012. Mechanisms of host receptor adaptation by severe acute respiratory syndrome coronavirus. J. Biol. Chem. **287**:8904–8911.
38. **Yount B, et al.** 2003. Reverse genetics with a full-length infectious cDNA of severe acute respiratory syndrome coronavirus. Proc. Natl. Acad. Sci. U. S. A. **100**:12995–13000.
39. **Zhang CY, Wei JF, He SH.** 2006. Adaptive evolution of the spike gene of SARS coronavirus: changes in positively selected sites in different epidemic groups. BMC Microbiol. **6**:88.
40. **Zhang MY, et al.** 2010. Potent and broad neutralizing activity of a single chain antibody fragment against cell-free and cell-associated HIV-1. MAbs **2**:266–274.
41. **Zhang MY, et al.** 2004. Improved breadth and potency of an HIV-1-neutralizing human single-chain antibody by random mutagenesis and sequential antigen panning. J. Mol. Biol. **335**:209–219.
42. **Zhao GP.** 2007. SARS molecular epidemiology: a Chinese fairy tale of controlling an emerging zoonotic disease in the genomics era. Phil. Trans. R. Soc. Lond. B Biol. Sci. **362**:1063–1081.
43. **Zhu Q, et al.** 2011. Analysis of respiratory syncytial virus preclinical and clinical variants resistant to neutralization by monoclonal antibodies palivizumab and/or motavizumab. J. Infect. Dis. **203**:674–682.
44. **Zhu Z, et al.** 2007. Potent cross-reactive neutralization of SARS coronavirus isolates by human monoclonal antibodies. Proc. Natl. Acad. Sci. U. S. A. **104**:12123–12128.